Food Chemistry: X 25 (2025) 102194

Contents lists available at ScienceDirect

Food Chemistry: X

journal homepage: www.sciencedirect.com/journal/food-chemistry-x

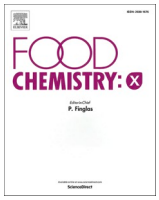

Inhibition of carboxymethyllysine in walnut cookies via food additives

Wenfeng Han [a,*], Po Qiu [b], Songtao Ge [a], Taoying Wei [a]

[a] Rice Wine College, Zhejiang Industry Polytechnic College, 151Qutun Road, Shaoxing 312000, China
[b] Shaoxing Liangshan Health Technology Co., Ltd, 368 Qutun Road, Shaoxing 312099, China

ARTICLE INFO

Keywords:
Walnut cookies
Food additives
Inhibition
Carboxymethyllysine
Sensory evaluation

ABSTRACT

Carboxymethyllysine(CML) is one of advanced glycation end products(AGEs), which is associated with the occurrence and development of chronic diseases such as diabetes, cardiovascular disease, Alzheimer's disease, etc. This study focused on assessing the CML formation pattern in walnut cookies and the related impact of food additives on the CML content and sensory characteristics. The results showed that the baking conditions significantly affected the CML content in the walnut cookies, which exhibited a significant positive correlation with the sensory evaluation scores. Three food additives, namely propyl gallate (PG), theaflavins (TF), and tea polyphenols (TP), were selected based on their high CML inhibition rates. They were combined using mixture optimal design, and the optimal compounding ratios were obtained, which were $X_1 = 0.236$, $X_2 = 0.400$, and $X_3 = 0.364$. These ratios were converted to the additive ratios in the walnut cookies, with PG at 0.0236 ‰, TF at 0.160 ‰, and TP at 0.146 ‰. The CML inhibition rate reached a maximum value of 40.98 %, with the sensory evaluation score also higher.

1. Introduction

Walnut cookies are a traditional Chinese confectionery. Wheat flour, fat, sugar, eggs, and other miscellaneous ingredients are mixed to form a malleable dough, which is molded and baked. These cookies are fluffy, sweet, and fragrant and are highly popular with consumers due to their affordability (Pan et al., 2020). However, the high sugar, fat, and protein levels in walnut cookies, as well as the baking process at high temperatures, promote the occurrence of the Maillard reaction, resulting in a significant accumulation of advanced glycation end products (AGEs). Studies have shown that AGEs accumulation in the human body can cause the development of diseases such as diabetes (Wautier et al., 2003), cardiovascular disease (Hartog et al., 2007), atherosclerosis (Goh & Cooper, 2008; Ha et al., 2004), cataracts (Kumar et al., 2007), Alzheimer's disease (Stevens, 1998), and rapid human organ aging (Baynes, 2001). More than 20 AGEs have been identified, including carboxymethyllysine (CML), carboxyethyllysine (CEL), pyrraline, pentosidine, imidazole-lysine and other compounds. CML was the first AGEs compound to be isolated and identified and is the most prevalent type in food (Büser et al., 1987). The molecular formula of CML is $C_8H_{16}N_2O_4$. Fig. 1 illustrates its chemical structure, showing a relative molecular mass of 204.22 and CAS registry number: 5746-04-3. CML is a white crystal with no fluorescent properties and no cross-linking. It is hygroscopic with a melting point of 280 °C and is soluble in water and alcohol. CML can be stably stored in an inert atmosphere at a temperature of −20 °C. Compared with other AGEs, CML displays higher acid stability and is often chosen as a marker substance to assess AGEs toxicity, detection, formation, and inhibition. Therefore, this study selected CML as a representative AGEs substance to establish a strategy for inhibiting its formation in walnut cookies.

The substances currently used both domestically and abroad to examine the inhibition of CML in food products primarily include natural flavonoids and phenolic acids. Kim et al. (2011) showed that isoquercitrin and chrysin inhibited AGEs formation in a dose-dependent manner. Zhang et al. (2014) added naringenin, epicatechin, and chlorogenic acid to a glucose-casein glycosylation model heated at 120.0 °C for 2.0 h. The results showed that these polyphenolic compounds inhibited the formation of AGEs such as CML. Liu and Li (2015) found that quercetin, rutin, and epicatechin inhibited AGEs, such as CML, in a bovine serum protein-fructose mimetic reaction system. Li et al. (2017) indicated that lychee pericarp proanthocyanidins inhibited the formation of AGEs such as CML in whey protein-glucose and bovine serum albumin-glucose simulated physiological systems. Liu et al. (2018) revealed that six polyphenolic compounds, including resveratrol, proanthocyanidins, and chlorogenic acid, inhibited the CML in cookies to a certain extent. Silván et al. (2011) found that ferulic acid restricted

* Corresponding author.
E-mail address: 254870849@qq.com (W. Han).

https://doi.org/10.1016/j.fochx.2025.102194
Received 12 August 2024; Received in revised form 3 January 2025; Accepted 14 January 2025
Available online 18 January 2025

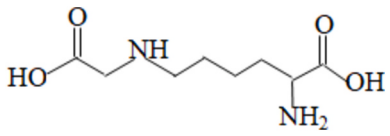

Fig. 1. Chemical structure of CML.

CML and fluorescent AGEs in a soybean globulin fructose system by 90 %. Pashikanti et al. (2010) indicated that 400 μmol/L of rutin metabolites (3,4-dihydroxyphenylacetic acid and 3,4-dihydroxytoluene) inhibited AGEs formation by 95 % and 90 %, respectively. Although most flavonoids and phenolic acids are natural active products with good inhibitory properties, they have not been approved as food additives. Their poor solubility and stability, as well as the unique color and odor of some, limit their use to only laboratory studies, significantly restricting practical application.

Propyl Gallate (PG), Theaflavins (TF) and Tea Polyphenols (TP) are food additives approved for use by the National Standard for Food Safety, Standard for Use of Food Additives (GB2760–2024). Wang et al. (2019) found that when the concentration of PG in the arginine- glucose simulation system was 0.5 mmol/L, its inhibition rates for glyoxal and methylglyoxal were 70.5 % and 67.6 %, respectively. Zhang (2017) found that theaflavins can directly bind and act on the bovine serum albumin-methylglyoxal simulation system, effectively inhibiting the formation of AGEs, and its inhibition effect was dose-dependent with theaflavins concentration. Zhou et al. (2018) found that the inhibition rate of CML by tea polyphenols in the bovine serum albumin-glucose simulation system was 13.67 %. Li (2016) found that epicatechin and epigallocatechin gallate can slow down the increase of free CML content in soy sauce, amino acid beverages, coconut juice, and corn juice during thermal processing, and the effect was better than the classical positive control aminoguanidine. The above results mainly focused on food additive monomers, CML precursor substances and simulation systems, and have not directly applied food additives to real food processing for study their inhibition effects on CML. This study directly applies food additives such as PG, TF and TP to the processing of walnut cookies for study their inhibition effects on CML. The research findings can be applied during actual walnut cookie production to reduce the CML levels, improve the consumption safety of these and other food products, and minimize the chronic diseases caused by the Maillard reaction.

2. Materials and methods

2.1. Materials and reagents

CML standard (98.0 % purity) and CML-D_4 isotope internal standard (98.0 % chemical purity, 97.9 % isotope purity) were supplied by TRC (Toronto, Canada). Acetonitrile and formic acid were mass spectra purity, supplied by Thermo Fisher Scientific (Waltham, MA, USA). The analytical reagents of formic acid (content ≥88.0 %) and methanol (content ≥99.5 %) were obtained from the Kemiou Chemical Reagent CO, Ltd. (Tianjin, China). Ammonia (content ≥25 %) was an analytical reagent from the Iron Tower Reagent Factory (Kaifeng, China). Ultra-purified water was prepared using a Milli-Q Advantage A10 system (Millipore, Bedford, MA, USA). PG、AG、TP were purchased from Shanxi Mixianer Biotechnology Co., Ltd. (Xi an, China); Antioxidant of bamboo leaves(*AB*)were purchased from Henan Yuzhong Biotechnology Co., Ltd. (Zhengzhou, China); TheaFlavins(TF) were purchased from Shanghai Ruixiang Biotechnology Co., Ltd. (Shanghai, China), all are at the level of food additives. Low gluten flour, shortening, sugar, eggs, baking powder were all purchased from the local supermarket.

2.2. Methods

2.2.1. Plotting of the standard curves

A series of CML standard solutions were prepared at concentrations of 1.0 ng/mL, 2.0 ng/mL, 5.0 ng/mL, 10.0 ng/mL, 20.0 ng/mL, and 50.0 ng/mL. Then, 10.0 ng/mL of the CML-D_4 internal standard solution was added to each concentration gradient, which was vortexed homogeneously and analyzed via ultra-high performance liquid chromatography-tandem mass spectrometry (UPLC-MS/MS) to determine the CML content. The response value Y (CML-D_4 concentration* (CML peak area/CML-D_4 peak area)) and CML concentration X were used as the vertical and horizontal coordinates, respectively, to plot the standard CML curve using the internal standard method. Next, the regression equation and correlation coefficient were calculated.

2.2.2. Method validation

Signal-to-noise ratio (S/N) refers to the ratio of signal intensity to baseline noise, which usually calculated from the chromatogram of the lowest concentration in the standard curve. The limit of detection (LOD) is defined as the concentration of $S/N = 3$(Hayashi et al., 1995), and the limit of quantitative (LOQ) is specified as the concentration of $S/N = 10$ (Chen et al., 2017). When S/N = X, then D = 3C/X. In this formula, C stands for the analyte concentration, X stands for S/N, and D stands for the LOD. When S/N = X, then Q = 10C/X. In this formula, C stands for the analyte concentration, X stands for S/N, and Q stands for the LOQ.

All quantitative detection methods need to be verified for accuracy. Therefore, a model sample system was established during the experiment for adding the standard test. The CML concentrations when adding the standard test were 15.0, 30.0, and 60.0 ng/mL, respectively. Six parallel tests were performed for each addition of the standard concentration. The calculation formula of the standard recovery rate is $P = \frac{(C_2 - C_1)}{C_0} \times 100\%$, In this formula, P is the standard recovery rate, C_2 is the detected value after adding the CML standard, C_1 is the background value, and C_0 is the added standard quantity.

Precision indicates the size of the random deviation and is usually expressed in terms of the relative standard deviation (RSD). It is the ratio of standard deviation (S) and the arithmetic mean of the detected results. $S = \sqrt{\frac{\sum_{i=1}^{n}(x_i - \bar{x})^2}{n-1}}$, $RSD = \frac{s}{\bar{x}} \times 100\%$. In this formula, S is the standard deviation, $\sum$ denotes sum, $\bar{\mathbf{x}}$ stands for the arithmetic mean, and $\sqrt{}$ stands for square root. Both the repeatability tests and the parallel tests were applied to evaluate the precision of the detection method during the experiment.

2.2.3. The walnut cookie recipes and production procedures

The basic recipe for the walnut cookies included 50.0 g of low-gluten flour, 30.0 g of shortening, 20.0 g of sugar, 5.0 g of egg, 5.0 g of water, and 2.0 g of baking powder. After the shortening was softened in water bath, it was added to the sugar and whipped until white in color and the volume expanded by SM-5 L mixer (Xinmai Machinery Co., Ltd.,Wuxi, China). The water and egg were added and stirred until homogeneous. Next, the sifted low-gluten flour was added to the whipped mixture and mixed at a slow speed until well blended. The dough was kneaded into long strips on a board and divided into 30.0 g portions, which were kneaded into rounds. The walnut cookies were arranged evenly on a baking sheet lined with oiled paper, leaving adequate gaps between them for expansion. The cookies were baked immediately for 20 min at 210 °C at the top and 180 °C at the bottom in SM2-523H baking chamber (Xinmai Machinery Co., Ltd.,Wuxi,China). The samples of this basic formula were used as a blank control group for the CML formation inhibition test.

The CML inhibition rate was calculated as follows:

$$\text{CML inhibition rate} = \left(1 - \frac{\text{CML content}_{\text{test}}}{\text{CML content}_{\text{blank}}}\right) \times 100\%$$

2.2.4. The effect of the baking conditions on the CML content and the sensory evaluation scores of the walnut cookies

The raw walnut cookies prepared in Section 2.2.3 were baked at the temperatures and durations presented in Table 1 to examine the effect of different baking conditions on the CML content and sensory evaluation scores of the final products.

2.2.5. Screening of the food additives

Here, 0.0112 g of PG, TF, TP, AG, and AB were separately dispersed in 5.0 g of water. The shortening was softened in water bath, after which the sugar was added and whipped until white in color and the volume expanded. Then, 5.0 g of each food additive dispersion was added to separate whipped samples, equating to a 0.10 ‰ content in the walnut cookies. Next, the egg was added and blended thoroughly, followed by the same steps described in Section 2.2.3.

2.2.6. Initial selection of the food additive compounding scheme

The three selected food additives were compounded. The National Standard for Food Safety, Standard for Use of Food Additives (GB2760–2024) stipulates that when food additives with the same function are used in mixture, the sum of the proportion of their respective dosages to the maximum dosage in the standard should not be more than 1. The three selected food additives are regarded as antioxidants since the maximum dosages in the walnut cookies included PG at 0.10 ‰ and TF and TP at 0.40 ‰ each. Table 2 shows the preliminary compounding scheme designed according to the usage requirements described above.

2.2.7. Food additive mixture optimal design

Since Scheffe proposed the simplex lattice design in 1958, the theory and practice of mixture optimal design have progressed significantly, playing a vital role in industry, agriculture, and scientific research (Draper et al., 2000; Scheffe, 1958). Design Expert 10.0.3 software is a professional experimental design software, which is powerful, easy to operate, and provides multiple design methods and tools. It can perform data analysis and model fitting optimization, reducing the number of actual experiments and improving efficiency. The working principle of the mixture optimal design function module was based on mathematical models and algorithms, treating three food additives as components in the mixture system, and the sum of the proportions of the three components was equal to 1. X_1 represented the PG proportion in the mix, X_2 denoted the TF proportion in the mix, and X_3 was the TP proportion in the mix. The upper and lower limits for the addition of each component were determined by considering the cost and the effect of action (Table 3). Using the mixture optimal design function module of Design Expert 10.03 software, test points were constructed based on the proportion and range limitations of each component, and 16 mixing schemes were designed (Table 4).

2.2.8. Sensory evaluation methods

Sensory quality evaluation is effective for accurately and objectively reflecting the quality of food. It is commonly used in food science research since no current instrumental tests can completely replace sensory evaluation. This study selected 10 professionally trained, experienced sensory assessors to form an evaluation team. The walnut cookie samples were assessed in a professional sensory quality evaluation room regarding morphology, color, organizational structure, and taste and scored out of 10. Table 5 lists the evaluation criteria.

The sensory quality evaluation protocol was reviewed and approved by Ethics Committee of Xinxiang Medical University(No: XYLL-20240001) and conformed to the ethical standards for medical research involving human subjects, as laid out in the 1964 Declaration of Helsinki and its later amendments. Participants provided written informed consent prior to taking part in the study.

2.2.9. Sample pretreatment

A 0.5000 g walnut cookie sample was ground to a particle size of approximately 0.5 mm, which was placed in a 10 mL polypropylene centrifuge tube. Then, 5.0 mL of n-hexane was added to the sample, vortexed to mix thoroughly, and centrifuged for 3.0 min at 4000 r/min,

Table 1
Baking temperature and time.

Top temperatures/°C Bottom temperatures /°C	Time /min
180 150	5.0、10.0、15.0、20.0、25.0
210 180	5.0、10.0、15.0、20.0、25.0
240 210	5.0、10.0、15.0、20.0、25.0

Table 2
The preliminary compounding scheme of food additives.

Test group	Amount of usage /‰		
	PG	TF	TP
I	0.05	0.2	–
II	0.05	–	0.2
III	–	0.2	0.2
IV	0.02	0.16	0.16

Table 3
Three factors mixing test design table.

Level	Factor		
	X_1	X_2	X_3
Low	0.2	0.2	0.2
High	0.4	0.4	0.4

Table 4
Mixture Optimal Design compound scheme for food additives.

Serial number	X_1	X_2	X_3
1	0.299	0.302	0.399
2	0.400	0.400	0.200
3	0.399	0.300	0.301
4	0.400	0.347	0.253
5	0.400	0.200	0.400
6	0.299	0.302	0.399
7	0.400	0.200	0.400
8	0.364	0.268	0.368
9	0.353	0.399	0.248
10	0.301	0.400	0.299
11	0.301	0.400	0.299
12	0.299	0.302	0.399
13	0.399	0.300	0.301
14	0.334	0.335	0.331
15	0.265	0.368	0.367
16	0.200	0.400	0.400

Table 5
Sensory evaluation criteria.

Item	Criteria	Score
Morphology	The shape is neat, the bottom surface is flat, the thickness is consistent, and the surface is uniform. Uniform cracking, no collapse, no skewing	2.0
Color	Natural yellowish-brown color, overall uniform color, slightly lighter color in the cracked recesses	2.0
Structure	Profile with uniform honeycomb voids, no charred particles, no impurities	2.0
Mouthfeel	Crisp and fluffy, moderately sweet, not greasy, pure flavor, no off-flavor	4.0

after which the n-hexane layer was discarded. The n-hexane degreasing process was repeated three times to remove the fat completely. Then, the sample was blow-dried with nitrogen at 60 °C by the N-EVAP-24 nitrogen-blowing instrument (Organomation, New York, NY, USA) to volatilize the n-hexane and obtain the degreased sample. Next, 500 μL of an acid protease solution at a concentration of 0.2 g/mL was added to the centrifuge tube containing the defatted sample. Then, 100 μL of the CML-D_4 isotope internal standard solution was added at a concentration of 2.5 μg/mL to provide a theoretical CML-D_4 concentration in the final solution of 10.0 ng/mL. This was followed by the addition of a phosphate buffer solution at pH 3 until reaching a volume of 4 mL. The tube was sealed and vortexed to mix thoroughly. The mixture was hydrolyzed in a water bath at 40 °C for 12 h while vortexing and mixing at 30.0 min intervals. The mixture was centrifuged at 4000 r/min for 3 min, and the supernatant was collected. Next, 5.0 mL of an aqueous formic acid solution at a concentration of 5.0 % was added to leach the residue, followed by vortex mixing and centrifugation at 4000 r/min for 3 min to obtain the supernatant. With 5.0 mL of the aqueous formic acid solution to leach for 3 times, all the supernatant obtained by total of 4 centrifugation were collected in a 25 mL volumetric flask, and diluted to 25 mL using a 5.0 % formic acid aqueous solution. The solution was passed once through filter paper to remove larger impurities and obtain the filtrate, which was considered the pretreated sample solution.

An MCX solid-phase extraction column (3.0 mL, 60.0 mg, 30.0 μm, Waters, USA) was used for sample purification in the VacElut SPS 24 vacuum SPE unit (Agilent Technologies, Santa Clara, CA, USA). The MCX column was activated with 3.0 mL of methanol and balanced with 3.0 mL of water, after which 1.0 mL of the sample solution was passed through the column at a rate of 1–2 drops/ s. After the sample solution was completely cleared from the system, the column was drenched with 3.0 mL of aqueous formic acid at a concentration of 5.0 % and vacuum-dried. Drenching was repeated with 3.0 mL of methanol, followed by vacuum drying, after which all the effluent solution was discarded. Finally, elution was performed with 5.0 mL of 15.0 % ammonia in methanol, followed by vacuum drying. The elution effluent was collected in a test tube and blow-dried with nitrogen at 60 °C. Finally, the residue in the test tube was dissolved with 1.0 mL of water, vortexed to mix, and passed through a 0.22 μm polyethersulfone needle filter in a 2.0 mL injection vial. A CML-D_4 isotopic internal standard and UPLC-MS/MS were employed to analyze and determine the CML content (Han et al., 2023).

2.2.10. UPLC-MS/MS detection method

The liquid phase chromatography instrument was an ACQUITY ultrahigh performance liquid chromatograph (Waters, Milford, MA, USA), and the chromatography column was an ACQUITY BEH Amide (2.1 mm × 100 mm, 1.7 μm, Waters, Milford, MA, USA). The protective column was an ACQUITY BEH Amide Vanguard column (1.7 μm, Waters, Milford, MA, USA). The mobile phases were phase A that consisted of an aqueous solution containing 0.1 % formic acid and phase B that contained acetonitrile, and the gradient elution parameters are shown in Table 6. Column temperature, injection volume, and running time were 35 °C, 2 μL, and 2 min, respectively.

The mass spectrometry instrument was an XEVO TQ-XS triple four-bar tandem mass spectrograph (Waters, Milford, MA, USA). The ion source was used in electrospray positive ion mode (ESI^+), while multi-response monitoring (MRM) denoted the monitoring mode. The capillary voltage, conical hole voltage, and source temperature were 3.0 kV, 25 V, and 150 °C, respectively, while the desolventizing gas temperature, desolventizing gas flow velocity, conical hole gas flow and collision energy were 400 °C, 700 L/h, 150 L/h and 17 V, respectively. The MRM mode included the quantitative analysis of daughter ion CML at *m/z* 205.22 – m/z 84.00, the qualitative analysis of daughter ion CML at m/z 205.22 – m/z 130.00, and the qualitative analysis of daughter ion at CML-D_4 m/z 209.00 – m/z 87.70.

Table 6
Gradient elution parameters.

Serial number	Time /min	Velocity of flow/(mL/min)	A /%	B /%
1	0.00	0.30	60.0	40.0
2	1.50	0.30	40.0	60.0
3	1.60	0.30	10.0	90.0
4	1.80	0.30	10.0	90.0
5	1.90	0.30	60.0	40.0
6	2.00	0.30	60.0	40.0

2.3. Statistical analysis method

Three parallel tests were conducted for each sample, and the test data were expressed in the form of "mean ± standard deviation." The significance of the test data was tested by Dunnett's T3 method of ANOVA in SPSS statistics 17.0. $p < 0.01$ indicates a highly significant difference between the compared data, $p < 0.05$ indicates that there is a significant difference and $p \geq 0.05$ indicates that there is no significant difference.

3. Results and discussion

3.1. Plotting of the standard curves

The internal standard curve of the CML was plotted using the response value *Y* and CML concentration *X* as the vertical and horizontal coordinates, respectively. The regression equation and correlation coefficient were calculated as follows: $Y = 1.9668\times + 0.1059$, $R^2 = 0.9998$, and the linear CML concentration ranged between 1.0 ng/mL and 50.0 ng/mL. Fig. 2(A) shows the total ion flow chromatogram of the CML, with a peak time of 1.01 min. Fig. 2(B) depicts the primary mass spectragram of the CML and CML—D_4, while Fig. 2(C) illustrates the secondary mass spectragram. The *m/z* of the quantitative CML daughter ion was 84.00, while that of the qualitative daughter ion was 130.00.

3.2. Method validation

The S/N (X) mean value was 83.29 of three 1.0 ng/mL CML parallel samples of the lowest concentration in the standard curve. According to $D = 3C/X$ and $Q = 10C/X$, the LOD and LOQ of CML via this detection method were approximately 0.036 ng/mL and 0.120 ng/mL, respectively. Therefore, it is evident that the LOD and LOQ are low, indicating the high sensitivity of this method.

The background value of the CML content was 32.3 ng/mL. The average recovery rates of CML adding standard of 15.0, 30.0, and 60.0 ng/mL were 92.46 %, 94.87 %, and 89.26 %, respectively. While the RSD ranged from 3.57 to 6.33 % as shown in Table 7. For accuracy in the methodological validation, acceptable recovery rates generally ranged from 80.0 to 120.0 % (Diaz et al., 2004). Therefore, the recovery rate of this method was within the acceptable range rendering it highly accurate.

The same sample was injected and analyzed six times within a short time. The average content over six injections was 32.5 ng/mL. According to the formula, the RSD value of the repeatability test was 3.86 %. The generally acceptable RSD range of precision is less than 10.0 %, and the RSD of this method is 3.86 %, which satisfies the precision requirements of repeatability tests. Six parallel samples were injected and analyzed. The average content over six injections was 32.3 ng/mL. According to the formula, the RSD value of the parallel test was 6.72 %. The generally acceptable RSD range of precision is less than 10.0 %. The RSD of this method is 6.72 %, which satisfies the precision requirements of parallel tests.

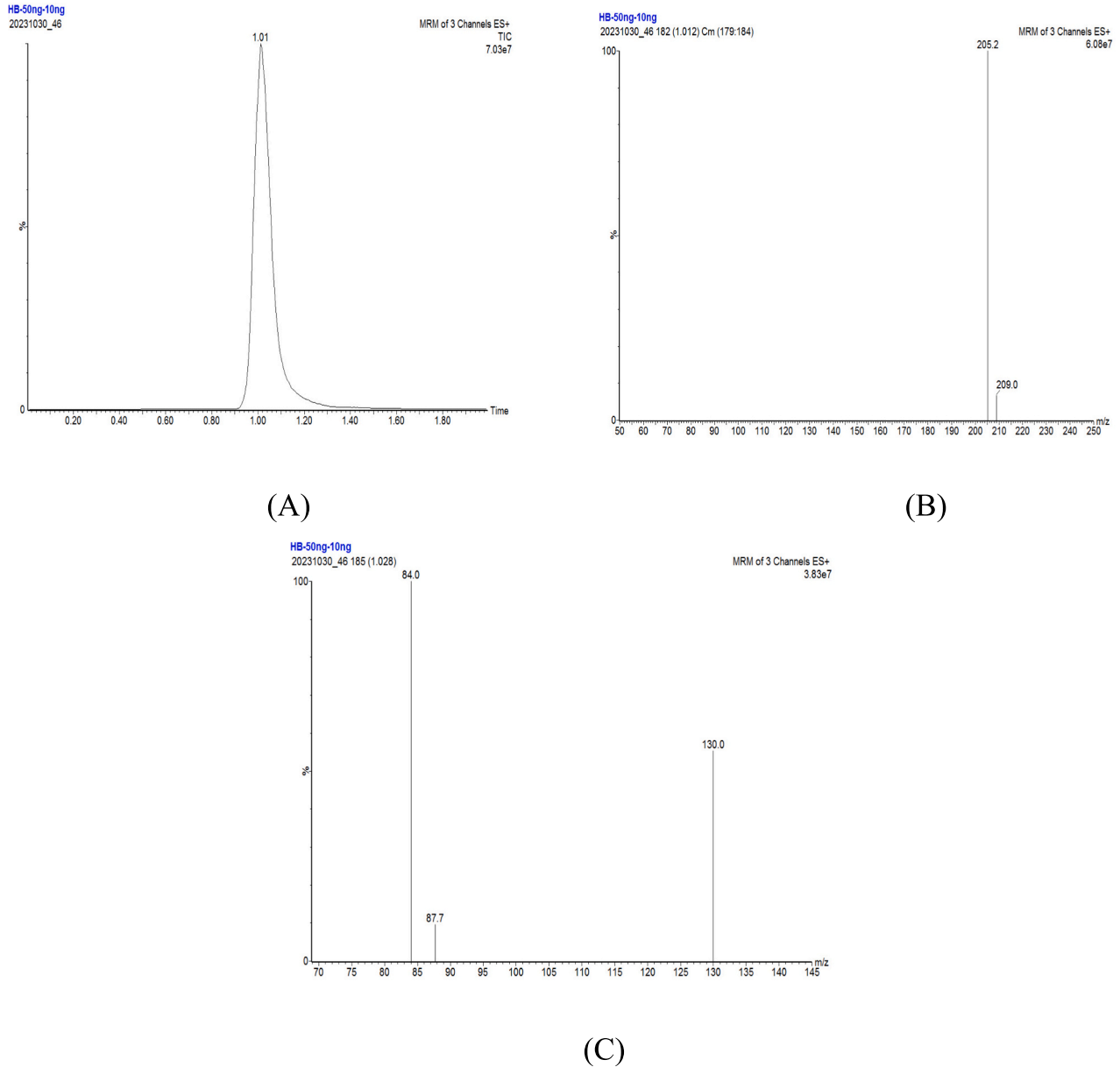

Fig. 2. The CML total ion flow chromatogram(A), the primary mass spectragram (B) and the secondary mass spectragram of CML and CML-D_4 (C).

Table 7
The adding standard recovery rate of CML.

Adding standard concentration (ng/mL)	Average recovery rate (%)	RSD (%)
15.0	92.46	6.33
30.0	94.87	3.57
60.0	89.26	4.58

3.3. The CML content in the walnut cookies in different baking conditions and its relationship with the sensory evaluation scores

Table 8 shows sensory evaluation results and CML content of walnut cookies under different baking conditions.the CML level and sensory evaluation score in the walnut cookies increased as the baking time was extended from 5.0 min to 25.0 min at lower temperatures of 180 °C (top) and 150 °C (bottom). At 25 min, the CML level and sensory evaluation score of the walnut cookies reached maximum values of (1954.80 ± 7.90) ng/g and (9.61 ± 0.21) points, respectively. The CML content and sensory evaluation score of the walnut cookies baked at temperatures of 210 °C (top) and 180 °C (bottom) initially increased as the baking time was extended, followed by a decrease, reaching maximum values of (1616.36 ± 6.70) ng/g and (9.40 ± 0.43) points, respectively, at 20.0 min. The CML content and sensory evaluation scores of the walnut cookies baked at higher temperatures of 240 °C (top) and 210 °C (bottom) also displayed an initial increase and a subsequent decline with extended baking time, reaching maximum values of (909.81 ± 4.60) ng/g and (8.24 ± 0.47), respectively, at 10.0 min. As illustrated in Fig. 3, the CML content and sensory evaluation scores of the walnut cookies exhibited a highly positive correlation. Furthermore, a higher CML level increased the sensory evaluation score. Han et al. (2021) also found that the frying process conditions of potato chips had a significant impact on the CML content, and the CML content was highly positively correlated with the sensory comprehensive score. Potato chips were fried at 180.0 °C, and the CML content and sensory evaluation scores showed a trend of first increasing and then decreasing with the prolongation of frying time. CML is a product of the Maillard reaction between reducing sugars and proteins. The formation and decomposition of CML occur simultaneously in the Maillard reaction, and high temperatures are more

Table 8
Sensory evaluation results and CML content of walnut cookies under different baking conditions.

Serial number	Top temperatures/°C Bottom temperatures /°C	Time/min	CML content /(ng/g)	Sensory evaluation score
1		5.0	282.33 ± 2.17^{c}	1.52 ± 0.13^{b}
2		10.0	841.88 ± 5.62^{g}	2.51 ± 0.47^{c}
3	180 150	15.0	1419.70 ± 7.89^{i}	6.16 ± 0.36^{f}
4		20.0	1670.59 ± 8.65^{k}	8.03 ± 0.19^{h}
5		25.0	1954.80 ± 7.90^{l}	9.61 ± 0.21^{i}
6		5.0	330.38 ± 2.56^{d}	2.23 ± 0.16^{c}
7		10.0	958.81 ± 4.24^{h}	5.95 ± 0.32^{f}
8	210 180	15.0	1441.40 ± 5.43^{i}	7.53 ± 0.60^{g}
9		20.0	1616.36 ± 6.70^{e}	9.40 ± 0.43^{i}
10		25.0	1551.78 ± 5.68^{j}	7.95 ± 0.16^{h}
11		5.0	632.43 ± 3.56^{e}	4.53 ± 0.38^{d}
12		10.0	909.81 ± 4.60^{h}	8.24 ± 0.47^{h}
13	240 210	15.0	746.81 ± 3.89^{f}	5.16 ± 0.10^{e}
14		20.0	212.07 ± 1.35^{b}	1.38 ± 0.25^{b}
15		25.0	67.50 ± 0.97^{a}	0.85 ± 0.07^{a}

Note: Different letters in the same column of data in the table indicate significant differences.
($p < 0.05$), while the same letters indicate insignificant differences ($p \geq 0.05$).

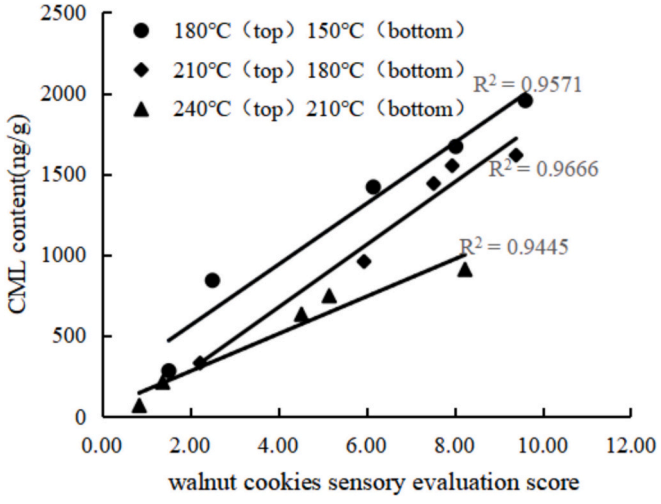

Fig. 3. Scatter plot of the correlation between sensory evaluation score of walnut cookies and CML content.

conducive to the decomposition of CML (Han et al., 2019). In the early stage of high-temperature baking treatment, the reaction substrate is sufficient, and the formation rate of CML is greater than the decomposition rate, resulting in a continuous increase in CML content. As the reaction progresses, the required reactants for CML formation decrease, and the rate of CML decomposition gradually exceeds the formation rate, thus the CML content also shows a decreasing trend (Lima et al., 2010).

As shown in Table 8, no significant differences were evident between the two higher sensory evaluation scores of (9.61 ± 0.21) and (9.40 ± 0.43), while the CML levels exhibited significant differences at (1954.80 ± 7.90) ng/g and (1616.36 ± 6.70) ng/g. Therefore, a CML content of (1616.36 ± 6.70) ng/g, the temperatures of 210 °C (top) and 180 °C (bottom) for 20 min were selected as the baking conditions for subsequent walnut cookie production.

3.4. Screening of the food additives

PG, TF, TP, AG, and AB were separately added to the walnut cookies to a content level of 0.10 ‰. As shown in Fig. 4, all five food additives restricted the CML content in the walnut cookies, with inhibition rates of (11.46 ± 1.02)%, (9.56 ± 0.85)%, (8.60 ± 0.68)%, (2.30 ± 0.06)%, and (0.81 ± 0.02)%, respectively. Wang et al. (2019) found that PG mainly inhibited CML generation by removing its precursors, including 1,2-carbonyl compounds, such as the highly active glycosylation factors glyoxal (GO) and methyl glyoxal (MGO). Hu et al. (2013) showed that TP inhibited the generation of AGEs such as CML in simulated food systems. Since the inhibitory effect of AG and AB was relatively small, this study selected PG, TF, and TP for combination to investigate their restrictive impact on the CML in walnut cookies.

3.5. Initial selection of the food additive compounding scheme

As shown in Table 9, among the four groups of protocols, I, II, and III belonged to a combination of two food additives, which showed CML inhibition rates of (26.69 ± 0.89)%, (24.35 ± 0.78)%, and (37.78 ± 0.56)%, respectively. Scheme IV is a combination of three food additives. Its inhibition rate was (40.51 ± 0.69)%. The results indicated that food additive combinations exhibited a synergistic effect. When multiple food additives with the same function are used together, the sum of their respective amounts to the maximum amount used in the standard should not exceed a ratio of 1, and the synergistic effect of the combination of three food additives is the largest. Huang and Xiong (2021) also found similar results, that is, the inhibition effect of the combination antioxidants of V_C palmitate, butylated hydroxyanisole (BHA) and Tert-Butylhydroquinone (TBHQ) on the peroxide value (POV) and acid value (AV) of rice bran oil is greater than that of any two of them.

The synergistic effect of PG, TF, and TP on CML inhibition in the walnut cookies reaction system of this experiment is based on the following reasons. PG played a leading role as it can quickly capture and eliminate free radicals, removing precursors of CML, weakening the initiation conditions of the Maillard reaction. TF interfered with the key steps of the Maillard reaction, reducing intermediate products that are converted to CML. TP not only chelated metal ions such as iron and copper to eliminate their catalytic effects, but also synergistically enhanced the overall antioxidant capacity with PG. When the three food additives were compounded, they each displayed their ability, closely cooperated, and blocked the generation pathway of CML in multiple dimensions, achieving a good inhibitory effect.

Therefore, this study used three food additives, namely PG, TF, and TP, to investigate the optimal formulation for CML inhibition in walnut cookies based on the mixture optimal design function of the Design Expert 10.0.3 data analysis software.

3.6. Results of the mixture optimal design

The CML content in the walnut cookies with added PG, TF, and TP based on the mixture optimal design was analyzed and determined via the sample pretreatment method described in Section 2.2.9 and the UPLC-MS/MS detection conditions delineated in Section 2.2.10, using CML-D_4 as an isotopic internal standard. Table 10 shows the results of the CML inhibitory rate and sensory evaluation score.

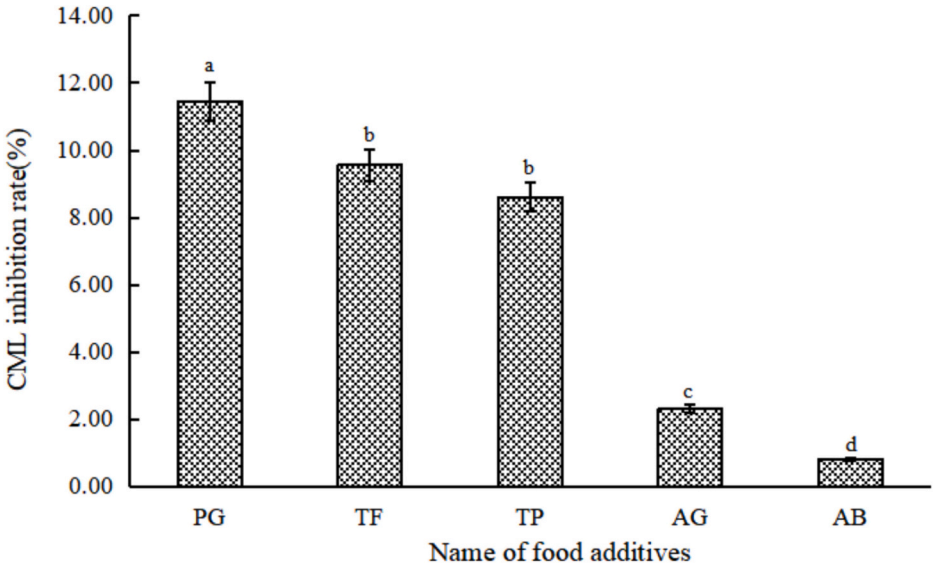

Fig. 4. The inhibition effect of food additives on CML in walnut cookies.
Note: Different letters in the figure indicate significant differences in data ($p < 0.05$), while the same letters indicate insignificant differences in data ($p \geq 0.05$).

Table 9
Compound scheme for food additives.

Compound scheme	Amount of usage /‰			CML inhibition rate/%
	PG	TF	TP	
I	0.05	0.2	–	26.69 ± 0.89^{b}
II	0.05	–	0.2	24.35 ± 0.78^{a}
III	–	0.2	0.2	37.78 ± 0.56^{c}
IV	0.02	0.16	0.16	40.51 ± 0.69^{d}

Note: Different letters in the same column of data in the table indicate significant differences.
($p < 0.05$), while the same letters indicate insignificant differences ($p \geq 0.05$).

Table 10
CML inhibition rate and sensory evaluation score based on Mixture Optimal Design.

Serial number	Factor			CML inhibition rate/%	Sensory evaluation score
	X_1	X_2	X_3		
1	0.299	0.302	0.399	35.86	9.40 ± 0.57^{a}
2	0.400	0.400	0.200	32.07	9.56 ± 0.89^{a}
3	0.399	0.300	0.301	17.85	9.43 ± 0.56^{a}
4	0.400	0.347	0.253	21.77	9.68 ± 0.70^{a}
5	0.400	0.200	0.400	18.73	9.81 ± 0.59^{a}
6	0.299	0.302	0.399	34.62	9.76 ± 0.48^{a}
7	0.400	0.200	0.400	18.10	9.32 ± 0.63^{a}
8	0.364	0.268	0.368	25.17	9.85 ± 0.54^{a}
9	0.353	0.399	0.248	37.74	9.50 ± 0.83^{a}
10	0.301	0.400	0.299	38.61	9.75 ± 0.62^{a}
11	0.301	0.400	0.299	40.83	9.53 ± 0.76^{a}
12	0.299	0.302	0.399	34.85	9.44 ± 0.80^{a}
13	0.399	0.300	0.301	18.35	9.36 ± 0.47^{a}
14	0.334	0.335	0.331	29.12	9.46 ± 0.69^{a}
15	0.265	0.368	0.367	37.41	9.58 ± 0.78^{a}
16	0.200	0.400	0.400	40.95	9.76 ± 0.51^{a}

Note: Different letters in the same column of data in the table indicate significant differences ($p < 0.05$), while the same letters indicate insignificant differences ($p \geq 0.05$).

3.6.1. Modeling and analysis of the CML inhibition rates

Multiple regression was applied and fitted to the experimental data in Table 10 using the Design Expert 10.0.3 data analysis software, with the CML inhibition rate as the response value. The following quadratic multinomial regression equation was obtained:

$$Y_{\text{CML inhibition rate}} = -348.815^{*} X_1 + 211.966^{*} X_2 + 222.515^{*} X_3 + 514.778^{*} X_1{}^{*} X_2 + 316.421^{*} X_1{}^{*} X_3 - 812.15^{*} X_2{}^{*} X_3$$

Table 11 shows the results of the regression ANOVA of the CML inhibition rate model. The regression model displayed high significance ($p < 0.01$), while the lack of fit was not significant ($p = 0.2135 > 0.05$), indicating adequate model fitting. Since the experimental values were relatively close to the predicted values, the model could be used to analyze and predict the CML inhibition rate. The model regression coefficient $R^2 = 0.9901$ and adjusted $R^2 = 0.9852$ indicated that 98.52 % of the data could be explained by the model, indicating the high reliability of the regression equation. As shown in Fig. 5, the measured CML inhibition rate was close to the predicted value, indicating good model fitting. Analysis of the variance results showed that the primary terms (X_1, X_2, and X_3) had a highly significant linear impact on the CML inhibition rate ($p < 0.01$), while the impact of its secondary term interaction (X_1X_2, X_1 X_3, and X_2X_3) was also substantial ($p < 0.01$).

3.6.2. The effect of the interaction between the factors on the CML inhibition rate

The response surface and contour plots obtained via the Design Expert 10.0.3 data analysis software were used to analyze the impact of each factor on the CML inhibition rate and the strength of the interaction between the factors. The incline of the response surface was positively correlated with the significance of the effect of each factor on the CML

Table 11
CML inhibition rate model and regression coefficient analysis results.

Source	Sum of squares	df	Mean square	F-value	*p*-value	
Model	1141.74	5	228.35	199.62	< 0.0001	**
Linear mixture	973.47	2	486.74	425.50	< 0.0001	**
AB	40.13	1	40.13	35.08	0.0001	**
AC	12.08	1	12.08	10.56	0.0087	**
BC	93.37	1	93.37	81.63	< 0.0001	**
Residual	11.44	10	1.14			
Lack of fit	7.78	5	1.56	2.13	0.2135	ns
Pure error	3.66	5	0.73			
Cor total	1153.18	15				
$R^2 = 0.9901$ Adj $R^2 = 0.9851$ Pre $R^2 = 0.9617$						

Note: $p < 0.01$ is extremely significant, represented by * *, $p < 0.05$ is significant, represented by *, $p \geq 0.05$ is not significant, represented by ns.

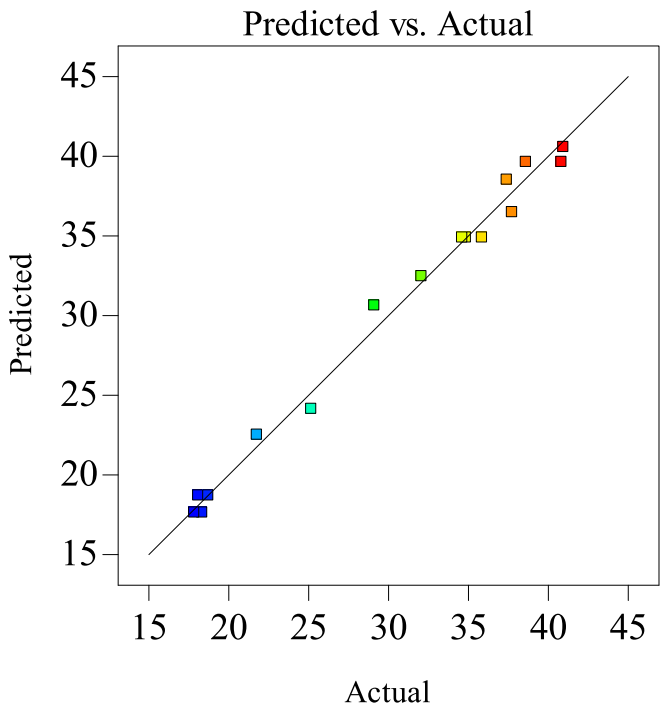

Fig. 5. CML inhibition rate actual value and predicted value graph.

inhibition rate. The shape of the contour lines and the density of the axis changes were related to the strength of the influence of each factor. As shown in Fig. 6, the CML inhibition rate decreased gradually as X_1 increased from 0.2 to 0.4 and was elevated when X_2 increased from 0.2 to 0.4. The CML inhibition rate displayed an initial decrease, followed by a gradual rise as X_3 increased from 0.2 to 0.4. The incline of the response surface and the sparseness of the contour lines were directly proportional to the influence of the factor on the response value. In comparison, the CML inhibition rate displayed more significant variation in the longitudinal span of the response surface and the gradient of the contour lines in the X_1 direction, followed by X_2. The influence of the three factors on the CML inhibition rate can be ordered as follows: $X_1>X_2>X_3$. Based on the results obtained via the Design Expert 10.0.3 software CML inhibition rate reached maximum value of 40.98 % when X_1 was 0.236, X_2 was 0.400, and X_3 was 0.364.

3.6.3. *Test result validation*

The Design Expert 10.0.3 software was used to predict the maximum CML inhibition rate of the different food additive proportions during walnut cookie production, values of 0.236 for X_1, 0.400 for X_2, and 0.364 for X_3 after three test replicates, and an average CML inhibition rate of 41.24 % (Table 12). The relative deviation was within 5 %, confirming the good correlation between the predicted and validated values.

4. Conclusions

This study investigates CML formation in walnut cookies in different baking conditions. The results indicate that extending the baking time from 5.0 min to 25.0 min increases the CML content and sensory evaluation scores of the walnut cookies baked at a top temperature of 180 °C and a bottom temperature of 150 °C. The CML levels and sensory evaluation scores of the walnut cookies baked at 210 °C (top) and 180 °C (bottom), as well as 240 °C (top) and 210 °C (bottom), display an initial rise, followed by a decline as the baking time is extended. A significant correlation is evident between the CML content and sensory evaluation scores of the walnut cookies. Higher CML levels increase the sensory evaluation scores. The baking conditions for walnut cookie production are determined based on the CML content and sensory evaluation scores. The top temperature is set at 210 °C, the bottom temperature at 180 °C, and the baking time is 20.0 min. The inhibition rates of the five food additives on the CML in the walnut cookies are ordered as follows: PG>TF>TP>AG>AB. This study selects three food additives, namely, PG, TF, and TP, due to their high CML inhibition rates. These food additives are combined based on a mixture optimal design. Optimal compounding ratios of X_1 (0.236), X_2 (0.400), and X_3 (0.364) are

Table 12
Mixture Optimal Design test verification results.

Serial number	X_1	X_2	X_3	CML inhibition rate/%	Sensory evaluation score
1	0.236	0.400	0.364	40.85	9.73
2	0.236	0.400	0.364	41.23	9.68
3	0.236	0.400	0.364	41.65	9.54
Mean value				41.24	9.65
Standard deviation				0.400	
RSD/%				0.970	

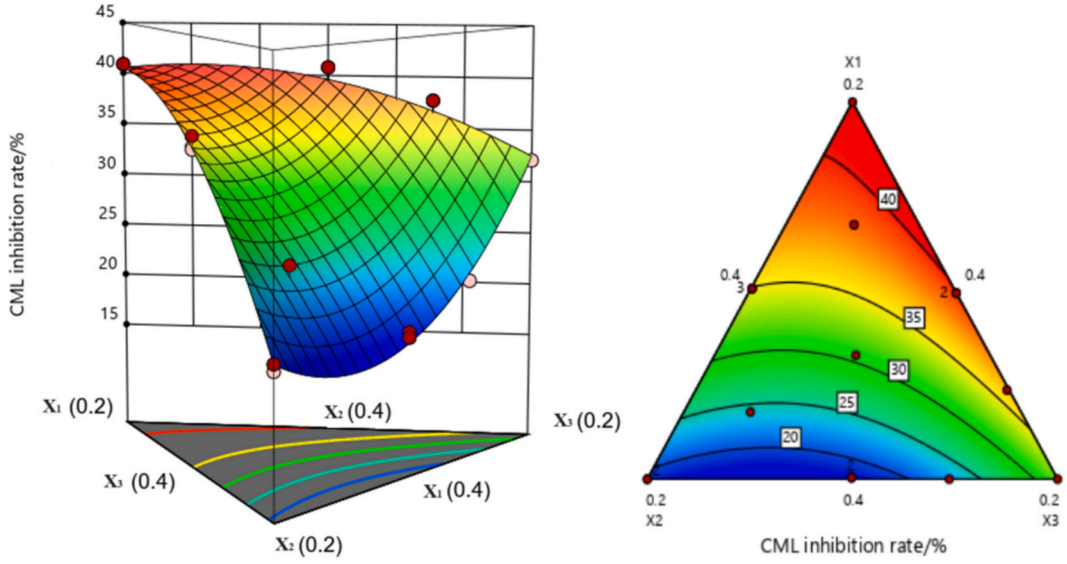

Fig. 6. The impact of the interaction of various factors on CML inhibition rate.

obtained and converted to the PG (0.0236 ‰), TF (0.160 ‰), and TP (0.146 ‰) additive ratios in the walnut cookies. The maximum CML inhibition rate value reached 40.98 % in these conditions, displaying higher sensory evaluation scores. If the results of this study are applied to the industrial production of walnut cookies, the product not only has a good taste, but also greatly reduces the CML content. It is suitable for everyone to consume, including the elderly, infants, and pregnant women.

Ethics declarations

Sensory quality evaluators mainly participated in sensory evaluation of walnut cookies and rated them based on their morphology, color, organizational structure, and taste. It is necessary to conduct ethical review on the sensory evaluation of walnut cookies. On the one hand, the evaluation involves inviting personnel to participate in the tasting, ensuring that participants are aware of the process, voluntarily participate, and safeguard their health and safety, and avoid potential risks. On the other hand, collecting evaluation data involves personal feelings and other privacy information. Ethical review can regulate the use of data, ensure its legality and compliance, prevent abuse, safeguard the rights and interests of participants, and make sensory evaluation scientific and ethical.

The sensory quality evaluation protocol was reviewed and approved by Ethics Committee of Xinxiang Medical University (No: XYLL-20240001) and conformed to the ethical standards for medical research involving human subjects, as laid out in the 1964 Declaration of Helsinki and its later amendments. Participants provided written informed consent prior to taking part in the study.

CRediT authorship contribution statement

Wenfeng Han: Writing – review & editing, Methodology. **Po Qiu:** Writing – original draft. **Songtao Ge:** Formal analysis. **Taoying Wei:** Methodology.

Declaration of competing interest

The authors declare that they have no known competing financial interests or personal relationships that could have appeared to influence the work reported in this paper.

Acknowledgements

This work was funded by high education institution visiting engineer school-enterprise cooperation project for the year 2023 of Zhejiang province education department (FG2023186) and science and technology plan project of Zhejiang Industry Polytechnic College (112709010921621040). The authors thankfully acknowledge the support received from the projects mentioned above.

Data availability

Data will be made available on request.

References

Baynes, J. W. (2001). The role of AGEs in aging: Causation or correlation. *Experimental Gerontology, 36*(9), 1527–1537. https://doi.org/10.1016/s0531-5565(01)00138-3

Büser, W., Erbersdobler, H. F., & Liardon, R. (1987). Identification and determination of N^{ε}-carboxymethyllysine by gas-liquid chromatography. *Journal of Chromatography A, 387*, 515–519. https://doi.org/10.1016/s0021-9673(01)94562-5

Chen, X. S., Zhu, S. X., Jiang, J. L., et al. (2017). Determination of maleic hydrazide residue in tobacco by HPLC-MS/MS. *Journal of Chinese Mass Spectrometry Society, 38*(2), 234–238. https://doi.org/10.7538/zpxb.youxian.2016.0044

Diaz, A., Vazquez, L. S., Ventura, F., et al. (2004). Estimation of measurement uncertainty for the determination of nonylphenol in water using solid-phase extraction and solid-phase microextraction procedures. *Analytica Chimica Acta, 506*, 71–80. https://doi.org/10.1016/j.aca.2003.10.083

Draper, N. R., Heiligers, B., & Pukelsheim, F. (2000). Kiefer ordering of simplex designs for second-degree mixture models with four or more ingredients. *Annals of Statistics, 28*(2), 578–590. https://doi.org/10.1214/aos/1016218231

Goh, S. Y., & Cooper, M. E. (2008). The role of advanced glycation end products in progression and complications of diabetes. *The Journal of Clinical Endocrinology & Metabolism, 93*(4), 1143–1152. https://doi.org/10.1210/jc.2007-1817

Ha, T. S., Song, C. J., Lee, J., & H.. (2004). Effects of advanced glycosylation endproducts on perlecan core protein of glomerular epithelium. *Pediatric Nephrology, 19*(11), 1219. https://doi.org/10.1007/s00467-004-1590-1

Han, W. F., Hua, X. M., & Tan, X. H. (2019). Formative regularity of N^{ε}-(1-Carboxymethyl)-L-lysine in lysine-glucose model reaction system of baked food. *Journal of the Chinese Cereals and Oils Association, 34*(12). https://doi.org/10.3969/j.issn.1003-0174.2019.12.008, 41-46+58.

Han, W. F., Qiu, P., & Zhang, L. (2023). Determination of N^{ε}-(1-Carboxymethyl)-L-lysine in brewing soy sauce by ultrahigh performance liquid chromatography coupled with tandem mass spectrometry. *Italian Journal of Food Science, 35*(4), 21–30. https://doi.org/10.15586/ijfs.v35i4.2393

Han, W. F., Zhou, Y. C., & Tan, X. H. (2021). Study on the formative regularity and inhibitory effect of CML in fried potato chips. *Journal of the Chinese Cereals and Oils Association, 36*(7), 69–76. https://doi.org/10.3969/j.issn.1003-0174.2021.07.013

Hartog, J. W. L., Voors, A. A., Schalkwijk, C. G., et al. (2007). Clinical and prognostic value of advanced glycation end-products in chronic heart failure. *European Heart Journal, 28*, 2879–2885. https://doi.org/10.1093/eurheartj/ehm486

Hayashi, Y., Matsuda, R., & Poe, R. B. (1995). Prediction of precision from signal and noise measurement in liquid chromatography: Limit of detection. *Chromatographia, 41*(1), 66–74. https://doi.org/10.1007/bf02274197

Hu, H. X., Fang, H. J., Zhang, S. F., et al. (2013). Inhibition the advanced glycation end products of food natural antioxidants in Vitr. *Journal of Chinese institute of. Food Science and Technology, 2013*(13), 15–20. https://doi.org/10.16429/j.1009-7848.2013.03.020, 3.

Huang, J., & Xiong, G. F. (2021). Optimization design of RSM for different antioxidant ratios in rice bran oil. *Jiangxi Nong Ye, 8*, 130–132+136.

Kim, H. Y., Lee, J. M., Yokozawa, T., et al. (2011). Protective activity of flavonoid and flavonoid glycosides against glucose-mediated protein damage. *Food Chemistry, 126*(3), 892–895. https://doi.org/10.1016/j.foodchem.2010.11.068

Kumar, P. A., Kumar, M. S., & Reddy, G. B. (2007). Effect of glycation on alpha-crystallin structure and chaperone-like function. *Biochemical Journal, 408*(2), 251–258. https://doi.org/10.1042/bj20070989

Li, S. Y., Qin, X. G., Huang, W., et al. (2017). Inhibitory effect of litchi pericarp procyanidins on maillard reactions in protein-based systems. *Modern Food Science and Technology, 33*(1), 68–73. https://doi.org/10.13982/j.mfst.1673-9078.2017.1.011

Li, Y. T. (2016). *Trapping and inhibition mechanisms of catechins on N^{ε}-(carboxymethyl) lysine*. Guangzhou: South China University of Technology.

Lima, M., Assar, S. H., & Ames, J. M. (2010). Formation of Nε-(carboxymethyl)lysine and loss of lysine in casein glucose-fatty acid model systems. *Journal of Agricultural and Food Chemistry, 58*(3), 1954–1958. https://doi.org/10.1021/jf903562c

Liu, H. C., & Li, J. X. (2015). Inhibitory effect of different inhibitor formation of advanced glycation Endproducts (AGEs) and advanced Lipoxidation Endproducts (ALEs) in vitro. *Journal of Chinese Institute of Food Science and Technology, 15*(10), 11–18. https://doi.org/10.16429/j.1009-7848.2015.10.002

Liu, H. L., Chen, X. M., Zhang, Y., et al. (2018). Inhibitory effects of polyphenolic compounds on N^{ε}-Carboxymethyl-lysine in biscuits. *Journal of Chinese Institute of Food Science and Technology, 18*(1), 95–103. https://doi.org/10.16429/j.1009-7848.2018.01.013

Pan, S. H., Wang, L. Z., Yan, D. M., et al. (2020). Application of Spanish mackerel (*Scomberomorus niphonius*) enzymatic hydrolysate in walnut cake. *Journal of Jiangsu Ocean University, 29*(1), 22–26.

Pashikanti, S., Alba, D. R. D., Boissonneault, G. A., et al. (2010). Rutin metabolites: Novel inhibitors of nonoxidative advanced glycation end products. *Free Radical Biology & Medicine, 48*(5), 656–663. https://doi.org/10.1016/j.freeradbiomed.2009.11.019

Scheffe, H. (1958). Experiments with mixture. *Journal of the Royal Statistical Society, 20*(2), 344–360.

Silván, J. M., Assar, S. H., Srey, C., et al. (2011). Control of the maillard reaction by ferulic acid. *Food Chemistry, 128*(1), 208–213. https://doi.org/10.1016/j.foodchem.2011.03.047

Stevens, A. (1998). The contribution of glycation to cataract formation in diabetes. *Journal of the American Optometric Association, 69*(8), 519–530.

Wang, J. Q., Xiao, L. B., Wang, X., et al. (2019). Scavenging effect of alkyl gallates on 1,2-dicarbonyl compounds in foods. *Food Science, 40*(19), 96–103. https://doi.org/10.7506/spkx1002-6630-20181008-033

Wautier, M. P., Massin, P., Guillausseau, P. J., et al. (2003). N (carboxymethyl)lysine as a biomarker for microvascular complications in type 2 diabetic patients. *Diabetes & Metabolism, 29*, 44–52. https://doi.org/10.1016/s1262-3636(07)70006-x

Zhang, J. (2017). *Neuroprotective effects of theaflavins on Alzheimer's disease model*. Changsha: hunan agricultural university.

Zhang, X. C., Hu, S. T., Chen, F., et al. (2014). Treatment of proteins with dietary polyphenols lowers the formation of AGEs and AGE-induced toxicity. *Food & Function, 5*(10), 2656–2661. https://doi.org/10.1039/c4fo00244j

Zhou, K. W., Chen, X. M., Liu, H. L., et al. (2018). The inhibition effects of polyphenols and flavonoids on advanced glycation end products. *Food Research and Development, 39*(4), 7–13. https://doi.org/10.3969/j.issn.1005-6521.2018.04.002